

Complex electronic structure of $\text{Ca}_{1-x}\text{Sr}_x\text{RuO}_3$

Kalobaran Maiti* and Ravi Shankar Singh†

Department of Condensed Matter Physics and Materials Science,
Tata Institute of Fundamental Research, Homi Bhabha Road, Colaba, Mumbai - 400 005, INDIA
(Dated: February 28, 2022)

We investigate the core level spectra of $\text{Ca}_{1-x}\text{Sr}_x\text{RuO}_3$ employing high resolution photoemission spectroscopy. Sample surface appears to be dominated by the contributions from Ru-O layers. Sr 3*p* core level spectra are sharp and asymmetric in SrRuO_3 as expected in a metallic system, and exhibit multiple features for the intermediate compositions that can be attributed to the difference in Ca-O and Sr-O covalency. The Ru core level spectra exhibit distinct signature of satellite features due to the finite electron correlations strength among Ru 4*d* electrons. The intensity of the satellite feature is weaker in the surface spectra compared to the bulk. The low temperature spectra exhibit enhancement of satellite intensity in the spectra corresponding to ferromagnetic compositions due to the inter-site exchange coupling induced depletion of the intensity at the Fermi level. The increase in *x* leads to a decrease in satellite intensity that has been attributed to the increase in hopping interaction strength due to the enhancement of the Ru-O-Ru bond angle. Evidently, the complex electronic properties of these materials are derived from the interplay between the electron correlation and hopping interaction strengths.

I. INTRODUCTION

4*d* and 5*d* transition metal oxides have drawn significant attention during last few decades due to the discovery of many interesting properties arising from the competition between electron-electron Coulomb repulsion (termed as ‘*electron correlation*’) induced effects, spin-orbit coupling and large crystal field effects. While 5*d* oxides exhibit signature of unusual transport and magnetic properties,^{1–3} 4*d* transition metal oxides, in particular Ru-based oxides exhibit plethora of interesting properties such as superconductivity,⁴ non-Fermi liquid behavior,^{5,6} unusual magnetic ground states^{5–8} etc. Even a simple perovskite compound, SrRuO_3 exhibits ferromagnetic long range order (Curie temperature, $T_C \sim 160$ K) despite having highly extended 4*d* character of the valence electrons.^{7,8} Another isostructural compound, CaRuO_3 exhibit complex ground state properties,⁹ with controversies on the existence of antiferromagnetic order,^{10–13} or the absence of any long-range order down to the lowest temperature studied.^{5,6,8,14} The behavior of CaRuO_3 is often discussed considering proximity to the quantum criticality.^{5,6}

Extensive studies have been carried out on these materials in the form of bulk samples and thin films. Photoemission studies suggest significantly different surface and bulk electronic structure,^{15,16} signature of particle-hole asymmetry,¹⁷ unusual thermal evolution of local structural disorder,¹⁸ unusual multiple features in the core level spectra of alkaline earth materials and oxygen as well,¹⁹ etc. In these systems, the conduction electrons consists of hybridized Ru 4*d* and O 2*p* states and moves via corner shared RuO_6 network. Hence, the tilting and buckling of the RuO_6 octahedra^{20–22} plays dominant role in deriving the electronic properties of this system. The Ru-O-Ru bond angles in SrRuO_3 are 167.6° and 159.7°, while those in CaRuO_3 are 149.6° - 149.8°. The electron hopping interaction strength and therefore the valence

band width, *W* is expected to be larger in SrRuO_3 than that in CaRuO_3 . Thus, the effective electron correlation strength, *U/W* (*U* = electron-electron Coulomb repulsion strength) is expected to be higher in CaRuO_3 than that in SrRuO_3 . This difference in *U/W* is often considered as the origin of the difference in ground state properties between these compounds, while some studies predicted similar *U/W* in these compounds. Evidently, the electronic properties in these compounds still remain to be a puzzle despite numerous studies. Here, we studied core level spectra of the whole series of compounds with formula, $\text{Ca}_{1-x}\text{Sr}_x\text{RuO}_3$ employing high resolution *x*-ray photoemission spectroscopy (XPS). Our results suggest interesting spectral evolution with temperature and composition, which could provide a clue to the understanding of the complex behavior of these materials.

II. EXPERIMENTAL

The samples of $\text{Ca}_{1-x}\text{Sr}_x\text{RuO}_3$ (for *x*=0.0, 0.2, 0.5, 0.7, 1.0) were prepared by conventional solid state reaction rout. High purity ingredients, CaCO_3 , SrCO_3 and RuO_2 were mixed in appropriate molar concentration, ground together for about an hour and calcined at 1273 K for about 24 hours and then treated at 1523 K. To achieve large grain size, the samples were sintered for about 72 hours in pellet form at the preparation temperature of 1523 K with two intermittent grounding. *X*-ray diffraction (XRD) patterns were recorded using Cu *Kα* line at every step. XRD patterns show orthorhombic crystal structure for all the samples with lattice constants similar to the observed values for single crystalline samples. It is to note here that the size of the single crystals are too small to carry out photoemission spectroscopy. It was almost impossible to grow samples of suitable size for the photoemission measurements and hence, highly sintered polycrystalline samples were used for these studies.

Direct current magnetic susceptibility measurements were performed using vibrating sample magnetometer (VSM). SrRuO_3 shows ferromagnetic transition at 165 K. Magnetic susceptibility, of $\text{Ca}_{1-x}\text{Sr}_x\text{RuO}_3$ reveals a broad ferromagnetic transition close to 150 K for all values of $x \geq 0.2$ [Ref.⁷]. μ_{eff} for all the samples in the paramagnetic region has been found to be close to the theoretical spin only value of $2.83\mu_B$ corresponding to $t_{2g}^3 t_{eg}^1$ occupation in Ru^{4+} .

Photoemission measurements were performed on *in situ* (base pressure better than 4×10^{-11} torr) scraped samples using an SES2002 Gammatdata Scienta analyzer. Reproducibility of the photoemission spectra and cleanliness of the sample surface was confirmed at each scraping trial. A high purity silver was also mounted on the same sample holder in electrical contact with other samples to determine the Fermi level. Measurements were carried out using different photon sources, at different temperatures. Total instrumental resolution was fixed to 0.8 eV for Mg $K\alpha$ and 0.3 eV for monochromatic Al $K\alpha$ photon energies.

III. RESULTS AND DISCUSSIONS

In Fig. 1, we show the spectral region for Ru 3d and Sr 3p core levels of $\text{Ca}_{1-x}\text{Sr}_x\text{RuO}_3$ for different values of x obtained using Al $K\alpha$ (circles) and Mg $K\alpha$ (solid lines) radiations at room temperature. Each spectrum exhibit multiple features - Sr 3p spin-orbit split signals appear around 268 eV and 278.5 eV binding energies indicating a spin-orbit splitting of about 10.5 eV for Sr 3p levels. Ru 3d features appear around 282 eV and 285.5 eV binding energies with a spin-orbit splitting of about 3.5 eV for Ru 3d levels. In order to investigate the Sr $3p_{1/2}$ contributions at the lower binding energy tail of the Ru 3d level, we have simulated the Sr $3p_{1/2}$ signal taking the experimental Sr $3p_{3/2}$ signal and the multiplicity ratio of 1:2. Here, the lineshape of the spectral function is kept same, which is a good approximation for such deep core levels and found to work well in the present case. The extraction procedure is demonstrated in Fig. 1(b) for a typical spectrum of SrRuO_3 exhibiting Ru 3d signal similar to that of CaRuO_3 , where there is no such signal present.

The intensity of Sr 3p signal with respect to the Ru 3d intensity increases gradually with the increase in Sr content in the sample as expected. The same spectral region collected with Mg $K\alpha$ radiations exhibit significantly different intensity ratio between Sr 3p and Ru 3d signals although the spectral lineshape seem to be similar at both the photon energies in a particular composition. This is shown by superimposing the Mg $K\alpha$ spectra over the Al $K\alpha$ spectra in Fig. 1(a). Clearly the integral intensity of the Ru 3d signal exhibit enhanced intensity in the Mg $K\alpha$ spectra relative to the intensity of the Sr 3p intensity. Two reasons can be thought for such intensity change - (i) photoemission cross section related change in intensity. The photoemission cross section²³

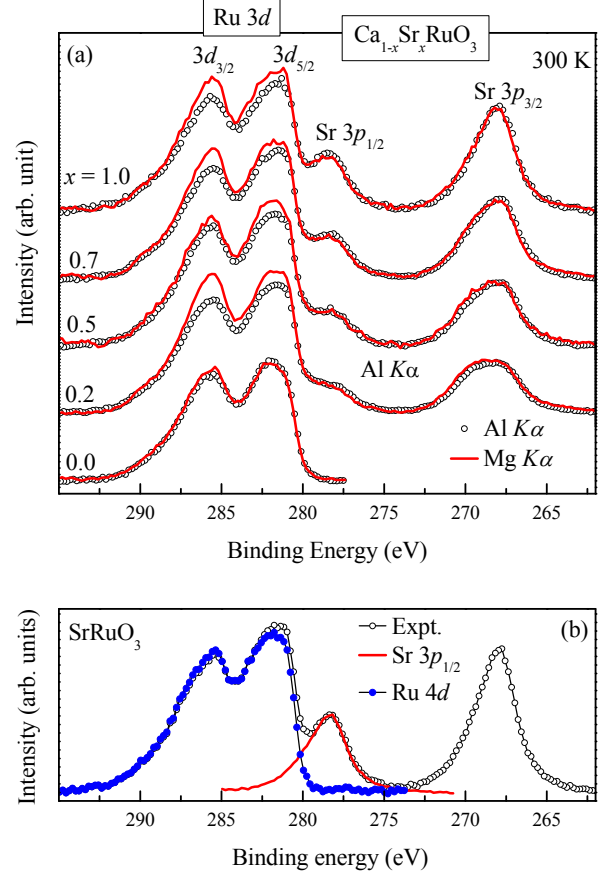


FIG. 1. (a) Ru 3d and Sr 3p core level spectra in $\text{Ca}_{1-x}\text{Sr}_x\text{RuO}_3$ for different values of x using Al $K\alpha$ (open circles) and Mg $K\alpha$ (solid lines) radiations at 300 K. (b) Ru 3d spectrum (closed circles) is extracted from the experimental spectrum (open circles) of SrRuO_3 after subtracting the Sr $3p_{1/2}$ contributions (solid line).

of Ru 3d and Sr 3p states are very similar at these two photon energies and hence can be ruled out here. (ii) The other possibility is the change in surface sensitivity - the surface sensitivity of the technique increases with the decrease in photon energy.²⁴ The enhancement of Ru 3d signal intensity with the increase in surface sensitivity suggests that the sample surface is dominated by Ru contributions. Thus, the oxygen coordination of surface Ru will be different from the bulk ones leading to different electronic structure, which is consistent with the earlier observations.¹⁵

In Fig. 2, we show the Ru 3d and Sr 3p spectral functions collected at 300 K and 20 K using Al $K\alpha$ radiations. Interestingly, the Sr 3p lineshape becomes narrower at 20 K compared to the 300 K spectra keeping the overall intensity of the features unchanged. However, Ru 3d spectra exhibit decrease in intensity in the $3d_{3/2}$ spectral region relative to the intensity in the $3d_{5/2}$ region. These spectral evolutions are unusual as the rel-

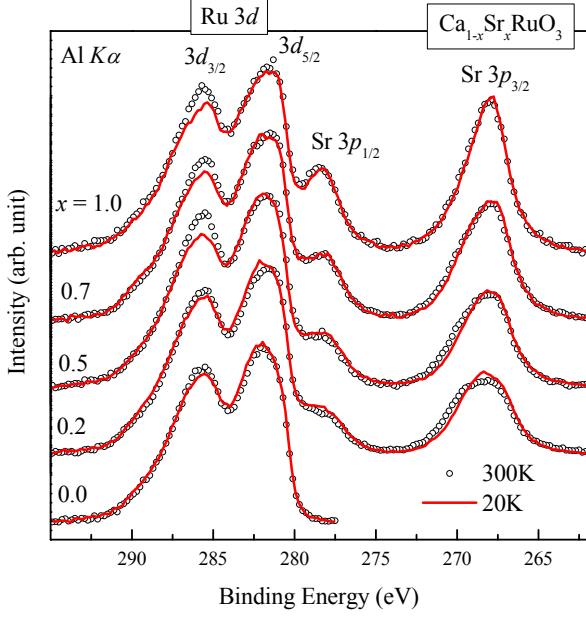


FIG. 2. Ru $3d$ and Sr $3p$ core level spectra in $\text{Ca}_{1-x}\text{Sr}_x\text{RuO}_3$ for different values of x collected using Al $K\alpha$ photon energy at 300 K (open circles) and 20 K (solid lines).

ative intensity ratio depends on the multiplicity of the corresponding levels - the multiplicity is not dependent on temperature. The relative spectral intensity change is possible only if there is additional contribution presumably due to $3d_{5/2}$ satellite appearing in the $3d_{3/2}$ spectral region and the satellite to main peak intensity ratio changes. Such possibility is also manifested by a shoulder at about 287.5 eV, which can be attributed to a satellite corresponding to the $3d_{3/2}$ photoemission signal. The spectral change appear to be most significant in the magnetically ordered compounds (SrRuO_3 end) compared to the paramagnetic compositions (CaRuO_3 end). The bulk valence band spectra also showed significant evolution with temperature in the magnetically ordered compounds, while the non-ordered compositions remained unchanged with temperature.²⁵ Magnetic ordering sets in due to the inter-site exchange interactions and thus, the electronic states mediating the inter-site exchange interactions are strongly coupled to the Ru-moment making it easier to screen the core hole in the photoemission final state that leads to larger intensity of the well screened feature.

Sr $3p$ spectra are shown in Fig. 3. Normalization by the intensity of the most intense feature exhibits narrowing of the spectral lineshape in the intermediate compositions while the end member, SrRuO_3 possess identical and sharp lineshape at both the temperatures studied. There is an additional feature marked by 'X' in the figure in the intermediate compositions that makes the features

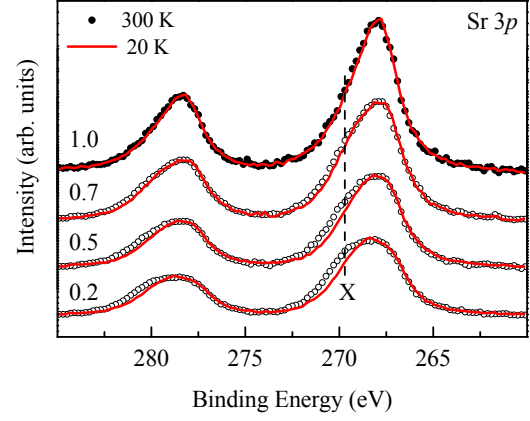


FIG. 3. Sr $3p$ core level spectra of $\text{Ca}_{1-x}\text{Sr}_x\text{RuO}_3$ for different values of x collected using Al $K\alpha$ photon energy at 300 K (open circles) and 20 K (solid lines). The Sr $3p_{1/2}$ spectral shape is approximated to be similar to the $3p_{3/2}$ lineshape.

broad. It has been found that Sr-O covalency is weaker than Ca-O covalency²⁶ that led to stronger distortion of the GdFeO_3 type orthorhombic distortion in CaRuO_3 . Thus, the Madelung potential of Sr surrounded by both Sr and Ca sites will be enhanced due to larger local distortion (the apical oxygens come closer to the Sr sites) relative to the Madelung potential at the Sr sites surrounded by only Sr ions. This explains appearance of an additional feature in the intermediate compositions at higher binding energy. Interestingly, decrease in temperature leads to a narrowing of the peaks - the two features come closer to each other presumably due to the weaker distortion in the thermally compressed structure at low temperatures.

Ru $3d$ spectra extracted by subtracting the Sr $3p_{1/2}$ contributions at the lower binding energy tail are shown in Fig. 4 for different photon energies and temperatures. All the spectra are normalized by the intensity of the most intense peak. Signature of five distinct features denoted by A, B, C, D and E are observed in all the spectra. While the two energy regimes below and above 284 eV binding energy can be attributed broadly to $3d_{5/2}$ and $2d_{3/2}$ spin-orbit split signals, the two feature structure of each of the spin-orbit split components have been observed in many other ruthenates and shown to be associated with different final state effects in photoemission process arising due to screening of core hole by valence electrons^{16,27,28}.

The relative intensity of the feature A and B does not change with the change in photon energy and temperature. However, the overall intensity in the $3d_{3/2}$ spectral region increases with the decrease in temperature and reduces with the change in photon energy towards higher surface sensitivity. These observations suggest the exist-

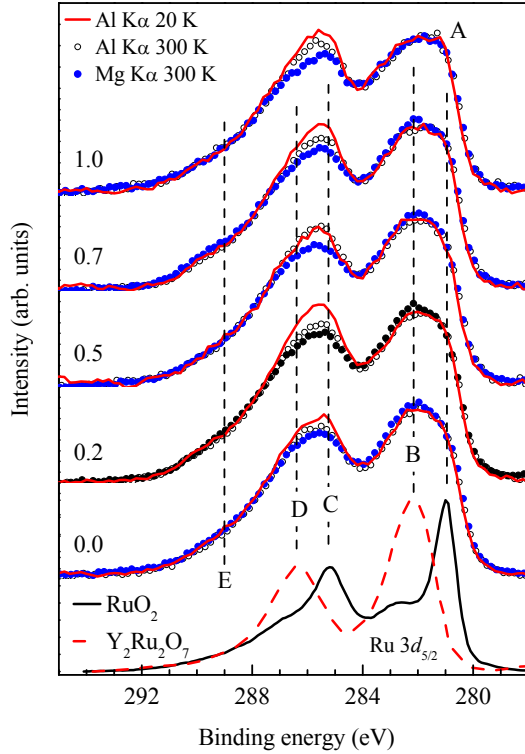


FIG. 4. Ru $3d$ core level spectra of $\text{Ca}_{1-x}\text{Sr}_x\text{RuO}_3$ for different values of x collected using Al $K\alpha$ (open circles) and Mg $K\alpha$ (solid line) photon energies at 300 K and Al $K\alpha$ photon energy at 20 K (solid symbols). The Sr $3P_{1/2}$ spectral contributions are subtracted out.

tence of a second satellite feature corresponding to $3d_{5/2}$ signal similar to the feature E for $3d_{3/2}$ signal increases at low temperatures and the surface spectra has weaker contribution. Since this feature correspond to another poorly screened feature, it is reasonable to state that the screening of the core level becomes less efficient at low temperatures and is stronger at the surface. In addition, the intensity of the feature A relative to the intensity of the feature B increases with the increase in x from $x = 0.0$ to 1.0 in $\text{Ca}_{1-x}\text{Sr}_x\text{RuO}_3$.

In Fig. 5, we show the Ru $3p$ core level spectra obtained at 20 K using Al $K\alpha$ radiations. Spectra shows spin orbit split two peaks at around 463.5 eV and 285.5 eV corresponding to photoemission signals from Ru $3p_{3/2}$ and Ru $3p_{1/2}$ electronic states, respectively. The spin orbit splitting of about 22 eV and the lineshape of the peaks are similar for all values of x . Weak satellite features representing the poorly screened final states appear around 13 eV higher binding energy with respect to the well screened (main) peak^{29–31}. The relative intensity of the satellite feature with respect to the intensity of the main peak is very small. Thus, the strength of the electronic interaction parameters are expected to be sig-

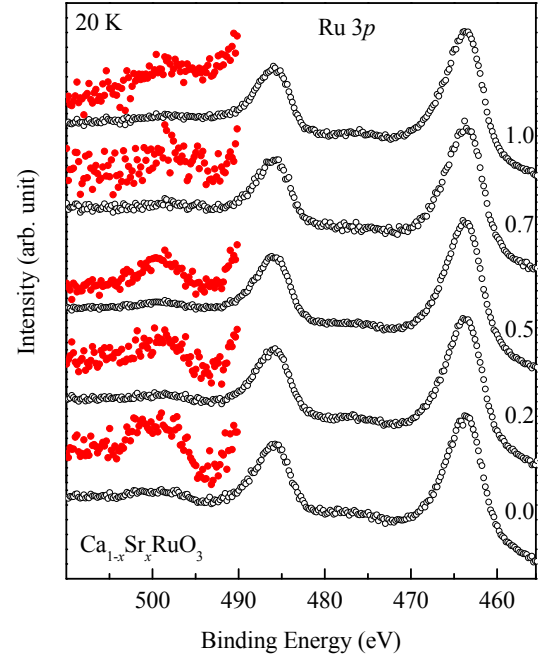


FIG. 5. Ru $3p$ core level spectra (open circles) obtained using Al $K\alpha$ radiations at 20 K. Satellite corresponding to $3p_{1/2}$ feature is shown in an expanded intensity scale (solid circles).

nificantly weak in these systems. The relative intensity of the satellite feature reduces gradually with the increase in x ; the ratio of the satellite to main peak intensities is about 20% in CaRuO_3 and 15% in SrRuO_3 . A careful look at the satellite signals reveals that there are two features as shown by rescaling the satellite feature at around 500 eV. The feature at higher binding energy in the satellite reduces continuously with the increase in x and becomes almost invisible in SrRuO_3 . Understanding of the origin of such spectral evolutions needs detailed calculations of the core level spectra. We hope, such calculations including all the electronic interaction parameters will be carried out in future to enlighten these interesting effects. Change in temperature does not have significant influence in the Ru $3p$ core level spectra.

Electron correlation leads to significant modification of the valence and conduction bands. The valence band of the correlated metallic transition metal oxides usually consists of two features³² - one feature appears at the Fermi level representing the delocalized electronic states and is known as *coherent feature*. The other one appears at higher binding energies derived by the electron correlation strength and represents the correlation induced electronic states. This feature is termed as the lower Hubbard band/*incoherent feature*. The electrons corresponding to the coherent feature are highly mobile and helps to screen the local positive charge present in the final state of photoemission. Thus, the core level spec-

tra often consists of at least two features - one the well screened feature and the other is the poorly screened feature.

In the Ru $3d$ spectra, the feature B, corresponds to the poorly screened core hole final state and the feature A can be attributed to the final state where the core hole is screened by the conduction electrons representing the coherent feature. This can be verified by the Ru $3d$ core level spectra of $\text{Y}_2\text{Ru}_2\text{O}_7$ (from Ref.²⁷) and RuO_2 (from Ref.²⁸) as shown in Fig. 4. RuO_2 is a good metal, where the influence of the correlation among the valence electron is negligible. On the other hand, $\text{Y}_2\text{Ru}_2\text{O}_7$ is a Mott insulator, where all the valence electrons contribute in the incoherent feature. It is evident from the figure that the peaks A and C correspond well to the $3d$ core level spectrum of RuO_2 and the features B and D correspond to the $3d$ spectra of $\text{Y}_2\text{Ru}_2\text{O}_7$. The signature of the feature E is not distinctly evident in the $3d$ spectra of RuO_2 or $\text{Y}_2\text{Ru}_2\text{O}_7$ spectra. More studies are required, in particular the studies based on theoretical calculations to reveal the origin of this feature.

Interestingly, Ru $3p$ spectra also exhibit signature of similar satellite structures in addition to the main peak due to the well screened final state. The distinct signature of the satellite features once again reaffirms the scenario based on various screening channels in these systems. In both, $3d$ and $3p$ spectra, the relative intensity of the satellite peak with respect to the main peak gradually reduces with the increase in Sr-concentration. Since, electron correlation strength is quite similar in both the systems, such spectral evolution can be attributed to the change in local crystal structure. CaRuO_3 possesses or-

thorhombic distortion and Ru-O-Ru angle is close to 150° , and SrRuO_3 is less distorted with Ru-O-Ru angle close to 65° . Increase in Ru-O-Ru bond angle enhances the hopping interaction parameter and hence screening of core hole becomes more efficient. The decrease in satellite intensity with the increase in x in both Ru $3d$ and $3p$ spectra can, thus, be attributed to the enhancement of Ru-O-Ru bond angle in this system.

IV. CONCLUSIONS

In summary, we studied the core level spectra of $\text{Ca}_{1-x}\text{Sr}_x\text{RuO}_3$ for various values of x employing photoemission spectroscopy. The surface appears to be dominated by Ru-O planes. The Sr core level spectra exhibit multiple feature in the intermediate compositions, which can be attributed to the differing Ca-O and Sr-O covalency. The Ru core level spectra exhibit distinct signature of satellite features due to finite electron correlation among Ru $4d$ valence electrons. The intensity of the satellite feature gradually decreases with the increase in Ru-O-Ru bond angle. Ferromagnetic compositions shows increase in satellite intensity at low temperatures that can be attributed to the depletion of intensity at the Fermi level due to inter-site exchange coupling leading to long range magnetic order.²⁵ The satellite intensity corresponding to the surface Ru core level spectra are weaker than those in the bulk. All the results manifest the complexity of the electronic structure due to the interplay between electron correlation and electron hopping interaction strength.

* Corresponding author: kbmaity@tifr.res.in

† Present Address: Indian Institute of Science Education and Research, Bhopal ITI (Gas Rahat) Building, Govindpura, Bhopal - 462 023, India

¹ G. Cao, J.E. Crow, R.P. Guertin, P.F. Henning, C.C. Homes, M. Strongin, D.N. Basov, and E. Lochner, *Solid State Commun.* 113 (2000) 657; K. Maiti, *Phys. Rev. B* 73 (2006) 115119; K. Maiti, R. S. Singh, V. R. R. Medicherla, S. Rayaprol and E.V. Sampathkumaran, *Phys. Rev. Lett.* 95 (2005) 016404.

² B.J. Kim, H. Jin, S.J. Moon, J.-Y. Kim, B.-G. Park, C.S. Leem, J. Yu, T.W. Noh, C. Kim, S.-J. Oh, J.-H. Park, V. Durairaj, G. Cao, and E. Rotenberg, *Phys. Rev. Lett.* 101 (2008) 076402.

³ R.S. Singh, V.R.R. Medicherla, Kalobaran Maiti, and E.V. Sampathkumaran, *Phys. Rev. B* 77 (2008) 201102(R); K. Maiti, *Solid State Commun.* 149 (2009) 1351.

⁴ Y. Maeno, H. Hashimoto, K. Yoshida, S. Nishizaki, T. Fujita, J. G. Bednorz, and F. Lichtenberg, *Nature* 372 (1994) 532.

⁵ P. Khalifah, I. Ohkubo, H. Christen, and D. Mandrus, *Phys. Rev. B* 70 (2004) 134426; Y. S. Lee, Jaeyun Yu, J. S. Lee, T. W. Noh, T.-H. Gimm, Han-Yong Choi, and C. B. Eom, *Phys. Rev. B* 66 (2002) 041104(R).

⁶ L. Klein, L. Antognazza, T.H. Geballe, M.R. Beasley, and A. Kapitulnik, *Phys. Rev. B*, 60 (1999) 1448.

⁷ R.S. Singh, P.L. Paulose, and K. Maiti, *Solid State Physics: Proceedings of the DAE Solid State Physics Symposium* 49 (2004) 876.

⁸ G. Cao, S. McCall, M. Shepard, J.E. Crow, and R.P. Guertin, *Phys. Rev. B*, 56 (1997) 321.

⁹ S. Tripathi, R. Rana, S. Kumar, P. Pandey, R. S. Singh, and D. S. Rana, *Sci. Rep.* 4 (2014) 3877; S. Middey, P. Mahadevan, and D. D. Sarma, *Phys. Rev. B* 83 (2011) 014416.

¹⁰ R. Vidya, P. Ravindran, A. Kjekshus, H. Fjellvag, and B.C. Hauback, *J. Solid State Chem.* 177 (2004) 146.

¹¹ A. Callaghan, C.W. Moeller, and R. Ward, *Inorg. Chem.* 5, 1572 (1966).

¹² J.M. Longo, P.M. Raccach, and J.B. Goodenough, *J. Appl. Phys.* 39 (1968) 1327.

¹³ T. Sugiyama and N. Tsuda, *J. Phys. Soc. Jpn.* 68 (1999) 3980.

¹⁴ J.L. Martinez, C. Prieto, J. Rodriguez-Carvajal, A. de Andrés, M. Valet-Regi, and J.M. Gonzalez-Calbet, *J. Magn. Magn. Mater.* 140-144 (1995) 179.

¹⁵ K. Maiti and R.S. Singh, *Phys. Rev. B* 71 (2005) 161102(R).

- ¹⁶ M. Takizawa, D. Toyota, H. Wadati, A. Chikamatsu, H. Kumigashira, A. Fujimori, M. Oshima, Z. Fang, M. Lippmaa, M. Kawasaki, and H. Koinuma, Phys. Rev. B 72 (2005) 060404(R).
- ¹⁷ K. Maiti, R. S. Singh, and V. R. R. Medicherla, Europhys. Lett. 78 (2007) 17002.
- ¹⁸ D. Lahiri, T. Shibata, S. Chattopadhyay, S. Kanungo, T. Saha-Dasgupta, R.S. Singh, S.M. Sharma, and K. Maiti, Phys. Rev. B 82 (2010) 094440.
- ¹⁹ R.S. Singh and K. Maiti, Phys. Rev. B 76 (2007) 085102; R. S. Singh and K. Maiti, Solid State Comm. 140 (2006) 188.
- ²⁰ M. V. Rama Rao, V. G. Sathe, D. Sornadurai, B. Panigrahi, and T. Shripathi, J. Phys. Chem. Solids 62 (2001) 797.
- ²¹ H. Nakatsugawa, E. Iguchi, and Y. Oohara, J. Phys.: Condens. Mater 14 (2002) 415.
- ²² H. Kobayashi, M. Nagata, R. Kanno, and Y. Kawamoto, Mater. Res. Bull. 29 (1994) 1271.
- ²³ J. J. Yeh, and I. Lindau, At. Data Nucl. Data Tables 32 (1985) 1.
- ²⁴ K. Maiti, U. Manju, S. Ray, P. Mahadevan, I. H. Inoue, C. Carbone, and D. D. Sarma, Phys. Rev. B 73 (2006) 052508; K. Maiti, A. Kumar, D. D. Sarma, E. Weschke, and G. Kaindl, Phys. Rev. B 70 (2004) 195112.
- ²⁵ R. S. Singh, V. R. R. Medicherla, and K. Maiti, Appl. Phys. Lett. 91 (2007) 132503.
- ²⁶ K. Maiti, Phys. Rev. B 73 (2006) 235110; K. Maiti, Phys. Rev. B 77 (2008) 212407.
- ²⁷ P. A. Cox, R. G. Egdellet, J. B. Goodenough, A. Hamnett, and C. C. Naishj, J. Phys. C: Solid State Phys. 16 (1983) 6221.
- ²⁸ H. -D. Kim, H. -J. Noh, K. H. Kim, and S. -J. Oh, Phys. Rev. Lett. 93 (2004) 126404.
- ²⁹ A. E. Bocquet, A. Fujimori, T. Mizokawa, T. Saitoh, H. Namatame, S. Suga, N. Kimizuka, Y. Takeda and M. Takano, Phys. Rev. B 45 (1992) 1561.
- ³⁰ A. E. Bocquet, T. Mizokawa, K. Morikawa, A. Fujimori, S. R. Barman, K. Maiti, D. D. Sarma, and Y. Tokura Phys. Rev. B 53 (1996) 1161.
- ³¹ A. Fujimori, M. Saeki, N. Kimizuka, M. Taniguchi and S. Suga, Phys. Rev. B 34 (1986) 7318.
- ³² A. Georges, G. Kotliar, W. Krauth, and M. J. Rozenberg, Rev. Mod. Phys. 68 (1996) 13; M. Imada, A. Fujimori, and Y. Tokura, Rev. Mod. Phys. 70 (1998) 1039.